Absorbing and reflecting sudden stratospheric warming events and their relationship with tropospheric circulation

Kunihiko Kodera, Hitoshi Mukougawa, Pauline Maury, Manabu Ueda, Chantal Claud

AGU PUBLICATIONS

JGR

Journal of Geophysical Research: Atmospheres

RESEARCH ARTICLE
10.1002/2015JD023359

Key Points:
- New classification of sudden stratospheric warming during the recovery phase
- Absorbing type warming events induce Arctic Oscillation on the surface
- Reflecting-type warming events produce a Pacific blocking

Supporting Information:
- Figure S1

Correspondence to:
K. Kodera,
kodera@stelab.nagoya-u.ac.jp

Citation:
Kodera, K., H. Mukougawa, P. Maury, M. Ueda, and C. Claud (2016), Absorbing and reflecting sudden stratospheric warming events and their relationship with tropospheric circulation, *J. Geophys. Res. Atmos.*, *121*, 80–94, doi:10.1002/2015JD023359.

Received 10 MAR 2015
Accepted 2 DEC 2015
Accepted article online 6 DEC 2015
Published online 7 JAN 2016

Absorbing and reflecting sudden stratospheric warming events and their relationship with tropospheric circulation

Kunihiko Kodera[1,2], Hitoshi Mukougawa[3], Pauline Maury[4], Manabu Ueda[3,5], and Chantal Claud[4]

[1]Institute for Space-Earth Environmental Research, Nagoya University, Nagoya, Japan, [2]Climate and Ecosystems Dynamics Division, Mie University, Tsu, Japan, [3]Disaster Prevention Research Institute, Kyoto University, Uji, Japan, [4]LMD/IPSL, CNRS, Ecole Polytechnique, Université Paris-Saclay, Palaiseau, France, [5]Now at Kobe Local Meteorological Office, JMA, Kobe, Japan

Abstract Sudden stratospheric warming (SSW) events have received increased attention since their impacts on the troposphere became evident recently. Studies of SSW usually focus on polar stratospheric conditions; however, understanding the global impact of these events requires studying them from a wider perspective. Case studies are used to clarify the characteristics of the stratosphere-troposphere dynamical coupling, and the meridional extent of the phenomena associated with SSW. Results show that differences in the recovery phase can be used to classify SSW events into two types. The first is the absorbing type of SSW, which has a longer timescale as well as a larger meridional extent due to the persistent incoming planetary waves from the troposphere. The absorbing type of SSW is related to the annular mode on the surface through poleward and downward migration of the deceleration region of the polar night jet. The other is the reflecting type. This is characterized by a quick termination of the warming episode due to the reflection of planetary waves in the stratosphere, which leads to an amplification of tropospheric planetary waves inducing strong westerlies over the North Atlantic and blocking over the North Pacific sector. Differences in the tropospheric impact of the absorbing and reflecting SSWs are also confirmed with composite analysis of 22 major SSWs.

1. Introduction

Sudden stratospheric warming (SSW) is a stratospheric phenomenon that occurs in the polar regions and is characterized by a rapid increase in temperature [*Scherhag*, 1952]. These events have received increased attention recently as the idea that changes in the stratospheric vortex can influence weather and climate in the troposphere has become accepted [*Thompson and Wallace*, 2001; *Baldwin and Dunkerton,* 2001].

The relationship between SSW and tropospheric blocking has also been revisited in recent studies [*Martius et al.,* 2009; *Woollings et al.,* 2010; *Nishii et al.,* 2011; *Bancalá et al.,* 2012; *Castanheira and Barriopedro*, 2010; *Barriopedro and Calvo*, 2014]. In fact, not only the vortex changes but also the wave reflection in the stratosphere can directly impact the troposphere through a change in planetary wave structure [*Perlwitz and Harnik*, 2003; *Shaw and Perlwitz*, 2010]. Note that planetary wave reflection and SSW events are considered to be two distinct stratospheric responses to the upward propagation of planetary waves into the stratosphere [*Perlwitz and Harnik*, 2004; *Harnik*, 2009; *Shaw and Perlwitz*, 2013]. *Harnik* [2009] considered that the difference between wave reflection and wave absorption events originates from the difference in the duration of tropospheric forcing. Here we will show that the duration of the forcing pulse (eddy heat flux at 100 hPa) can also be influenced by the stratospheric condition. *Kodera et al.* [2013] indicated that the planetary wave reflection can occur as a part of the life cycle of an SSW event following the maximum phase of the warming. In fact, some stratospheric warmings end prematurely due to the planetary wave reflection in the stratosphere, as will be shown later.

Downward propagation of planetary waves in the stratosphere associated with the wave reflection, or wave trapping, can also lead to amplification of tropospheric planetary waves, which in turn produces a favorable condition for blocking occurrence around an enhanced ridge of planetary waves, in particular over the North Pacific sector [*Kodera et al.,* 2008, 2013]. This causal relationship is also consistent with a study by *Bancalá et al.* [2012] showing an increase in the occurrence frequency of the Pacific blocking after the SSW. Some SSW events also significantly influence the equatorial lower stratosphere through equatorward propagation

of planetary waves, which induces upwelling and cooling there [e.g., *Ueyama et al.,* 2013; *Gómez-Escolar et al.,* 2014]. Such a tropical influence of SSW penetrates further down into the tropical troposphere through the modification and deepening of the convective activity in the tropical tropopause layer [*Kodera*, 2006; *Kodera et al.,* 2015; *Eguchi et al.,* 2015].

The duration of the warming varies considerably among SSW events. The mean duration of the polar warming in the lower stratosphere is about a month [*Limpasuvan et al.,* 2004]. However, there have been SSW events in which the warming quickly ends or is interrupted within about 10 days. What determines the duration of the SSW? It is commonly believed that the SSW ends following the decay of the tropospheric planetary waves [*Matsuno*, 1971]. However, an abrupt termination of the warming could arise from a change in wave propagation properties within the stratosphere.

SSW events are usually classified into major or minor warmings according to the degree of perturbation of the stratospheric polar vortex. Reversal of the westerly at 10 hPa and 60°N is usually taken as the definition of a major SSW event. However, not all major SSWs produce weakening of the tropospheric polar vortex [*Baldwin and Dunkerton*, 2001] nor do they produce cooling in the equatorial stratosphere [*Taguchi*, 2011]. SSW events have also been classified according to the dominant component of the zonal wavenumber (wave number 1 or 2) that led to the breakdown of the polar vortex [e.g., *Naujokat et al.,* 2002]. In recent studies, SSW events have been classified into vortex displacement and vortex splitting types according to the geometry of the deformed polar vortex [*Charlton and Polvani*, 2007; *Mitchell et al.,* 2013]. It should be noted that vortex splitting occurs during not only wave number 2 SSW, but also wave number 1 SSW events as shown in *Bancalá et al.* [2012] and *Barriopedro and Calvo* [2014]. This is because these two classifications are based on different aspects: wave numbers 1 and 2 classification focuses on the characteristics of the wave forcing that induces the SSW, whereas splitting-displacement classification is based on the stratospheric response to wave forcing.

SSW events can also be classified based on the subsequent tropospheric response. A statistical study by *Baldwin and Dunkerton* [1999] showed that the negative phase of the Arctic Oscillation (AO) or the surface signal of the Northern Annular Mode (NAM) tends to occur following an SSW or a weak stratospheric vortex event. However, this is not the case for all SSW events. For example, two major SSW events occurred during the boreal winter of 1999, and the weakened polar vortex did not descend to the troposphere in the first event, whereas in the second, the weakened polar vortex extended from the stratosphere to the troposphere as reported in *Baldwin and Dunkerton* [2001].

Differing tropospheric impacts of SSWs of the vortex displacement and splitting types have also been reported in recent studies [*Charlton and Polvani*, 2007; *Cohen and Jones*, 2011; *Kuttippurath and Nikulin*, 2012; *Mitchell et al.,* 2013]. However, their association with the NAM index is not stable, suggesting no significant correlation [*Charlton and Polvani*, 2007]. In addition, classification of the SSWs from the winter of 1999 according to the geometry of the polar vortex remains controversial. This is because *Charlton and Polvani* [2007] classified the SSW in December 1998 as a displacement type and that in February 1999 as a splitting type, whereas *Mitchell et al.* [2013] categorized the former SSW as a mixed type and the latter as a displacement type. Therefore, the difference in the tropospheric response of the two SSWs that developed in the winter of 1999 cannot be unequivocally defined based solely on the difference in the geometry of the stratospheric polar vortex.

The dominant component of the zonal wave number that characterizes the SSW does not necessarily determine the subsequent atmospheric response to the SSW. For example, the SSW in January 2010 was a wave number 1 type, but that in January 2009 was a wave number 2 type [*Ayarzagüena et al.,* 2011]. However, despite the different wave numbers, both SSW characterized by large warming events induced a similar atmospheric response, including weakening of the tropospheric polar vortex and a cooling in the equatorial stratosphere [*Kodera et al.,* 2015]. Thus, we must investigate the different aspects of SSW more closely, in particular the connection with the troposphere, and also identify what the essential features of these differences are.

The rest of this paper is organized as follows. Section 2 summarizes the data used, and the differences found among the various SSW events is described in section 3, beginning with the above-mentioned two SSWs from winter 1999. Then, the analysis is extended to SSWs from the four winters of 2007–2010, which had very different characteristics [*Martineau and Son*, 2013]. To allow coverage of a greater variety of SSW events, our

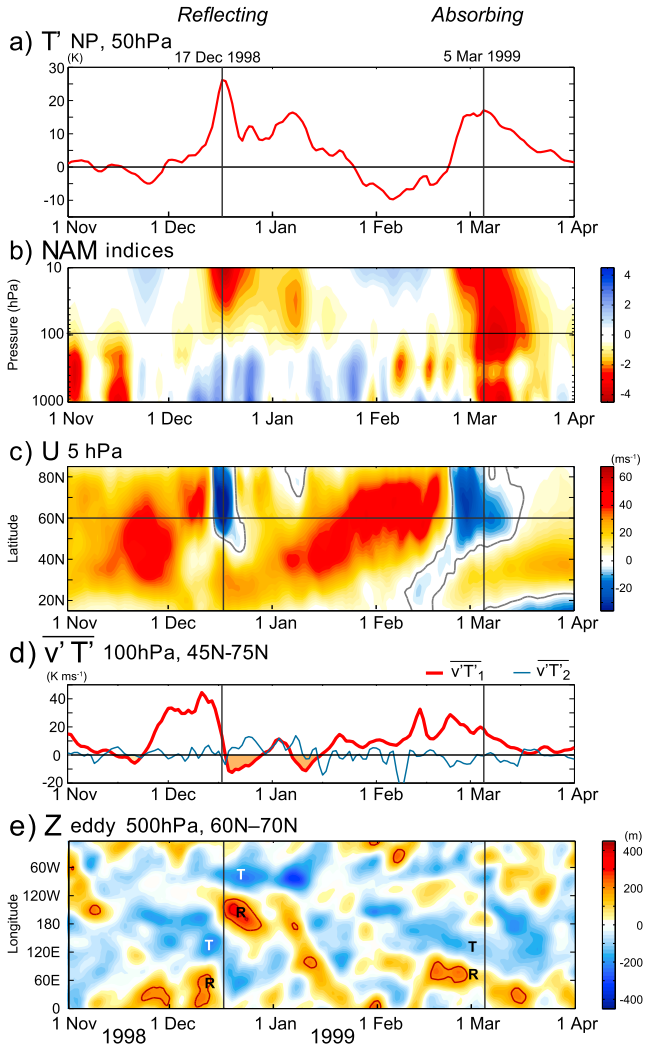

Figure 1. Evolution of atmospheric circulation from 1 December 1998 to 1 April 1999. (a) Anomalous north polar (80–90°N) temperature at 50 hPa. (b) Height-time section of NAM indices from *Baldwin and Dunkerton* [2001]. (c) Latitude-time section of 5 hPa zonal mean zonal wind. The zero contour is shown. (d) Eddy heat flux associated with zonal wave number 1 (red line) and wave number 2 (blue line) at 100 hPa averaged over 45–75°N. (e) Longitude-time section of zonally asymmetric component of 500 hPa geopotential height averaged over 60–70°N. Contours are 200 and 300 m. R and T indicate longitudinal positions of the main ridge and the trough around T_{max} (vertical lines), respectively.

analysis is supplemented by the well-documented SSW event of February 1979 [see *Andrews et al.,* 1987]. Finally, a discussion and concluding remarks are presented in section 4.

2. Data

We used the meteorological reanalysis data from the European Centre for Medium-Range Weather Forecasts (ECMWF) ERA-Interim [*Dee et al.,* 2011] for the period January 1979 to December 2013. The spatial resolution of this data set is 0.75° in latitude and 0.75° in longitude (approximately 80 km or T255) and has 60 vertical levels extending from the surface up to 0.1 hPa. The daily mean was obtained from the 6-hourly data set, and the climatology was defined as the mean of the 35 year study period (1979–2013). The NAM index used in the present study for the winter 1998/1999 was calculated by *Baldwin and Dunkerton* [2001] over 1000–10 hPa and was obtained from http://www.nwra.com/resumes/baldwin/nam.php.

3. Results

3.1. Winter 1999

Two major SSW events occurred during the winter of 1999 (the year of winter corresponds to that of January), one in mid-December 1998 and the other at the end of February 1999. The daily mean anomalous temperature at 50 hPa in the northern polar region (80–90°N) is shown in Figure 1a. *Baldwin and Dunkerton* [2001] noted that the negative NAM anomaly did not descend into the troposphere during the first SSW but did during the second event (Figure 1b). However, no consideration was given to the mechanism that caused the differing tropospheric responses associated with these two SSWs.

The meridional structure of the zonal mean zonal wind also differed considerably between the two SSW events. The latitude-time cross section of the 5 hPa zonal mean zonal wind (Figure 1c) shows that the deceleration of the westerly is limited to the north of 50°N for the first SSW, while during the second event the weakening of the westerly jet occurs over a wider latitudinal range, beginning in the tropics and then extending into the polar region.

Planetary wave forcing from the extratropical troposphere is monitored via the eddy heat flux at 100 hPa averaged over the extratropical Northern Hemisphere (NH; 45–75°N). Figure 1d shows the eddy heat flux associated with zonal wave numbers 1 (red line) and 2 (blue line). In both cases, the wave number 1

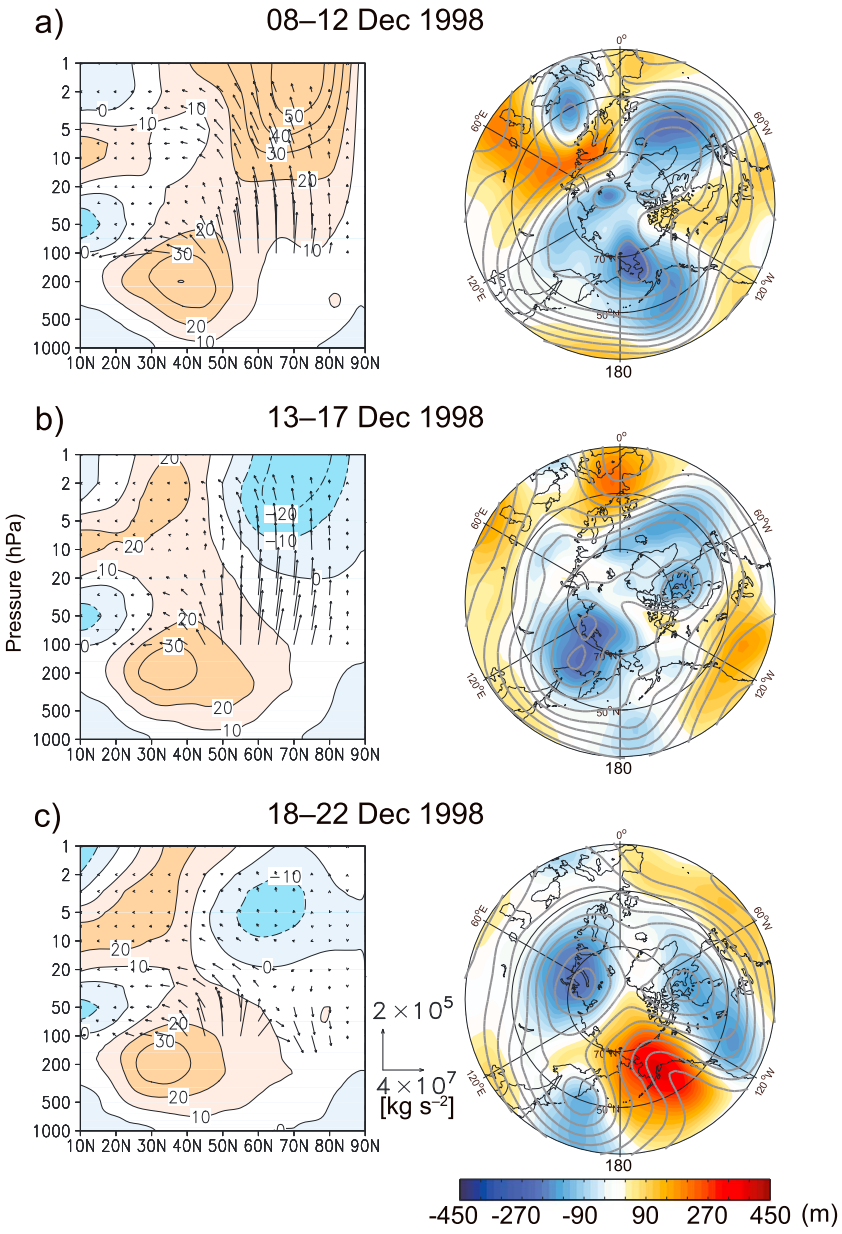

Figure 2. Five day mean E-P flux sections: shading contours and arrows indicate zonal mean zonal wind and E-P flux, respectively (left column). Five day mean 500 hPa geopotential height (contours) and its anomaly with respect to the climatology (color shading). (a) 8–12 December, (b)13–17 December, and (c)18–24 December 1998 (right column).

component plays a dominant role in initiating the SSW. However, a difference occurs during the end phase, in that the heat flux of the wave number 1 component suddenly becomes negative for the SSW in December 1998, but in February 1999, it decreases gradually over time. The sign of the eddy heat flux is related to the vertical component of Eliassen-Palm (E-P) flux, and hence negative absolute values of the former are related with downward propagation of waves. These changes in the vertical propagation of planetary waves around 16 December 1998 appear as a sudden alteration of a ridge associated with the tropospheric planetary wave from the European to the Pacific sector (Figure 1e). Such a sudden change in the tropospheric wave structure is not seen in the second SSW at the end of February 1999.

The different tropospheric connections between the two SSWs can be more easily seen in terms of the wave propagation properties. Figures 2 and 3 show the evolution of E-P flux and 500 hPa geopotential height from the onset date of the major warming (when the 10 hPa zonal mean zonal wind becomes easterly at 60°N),

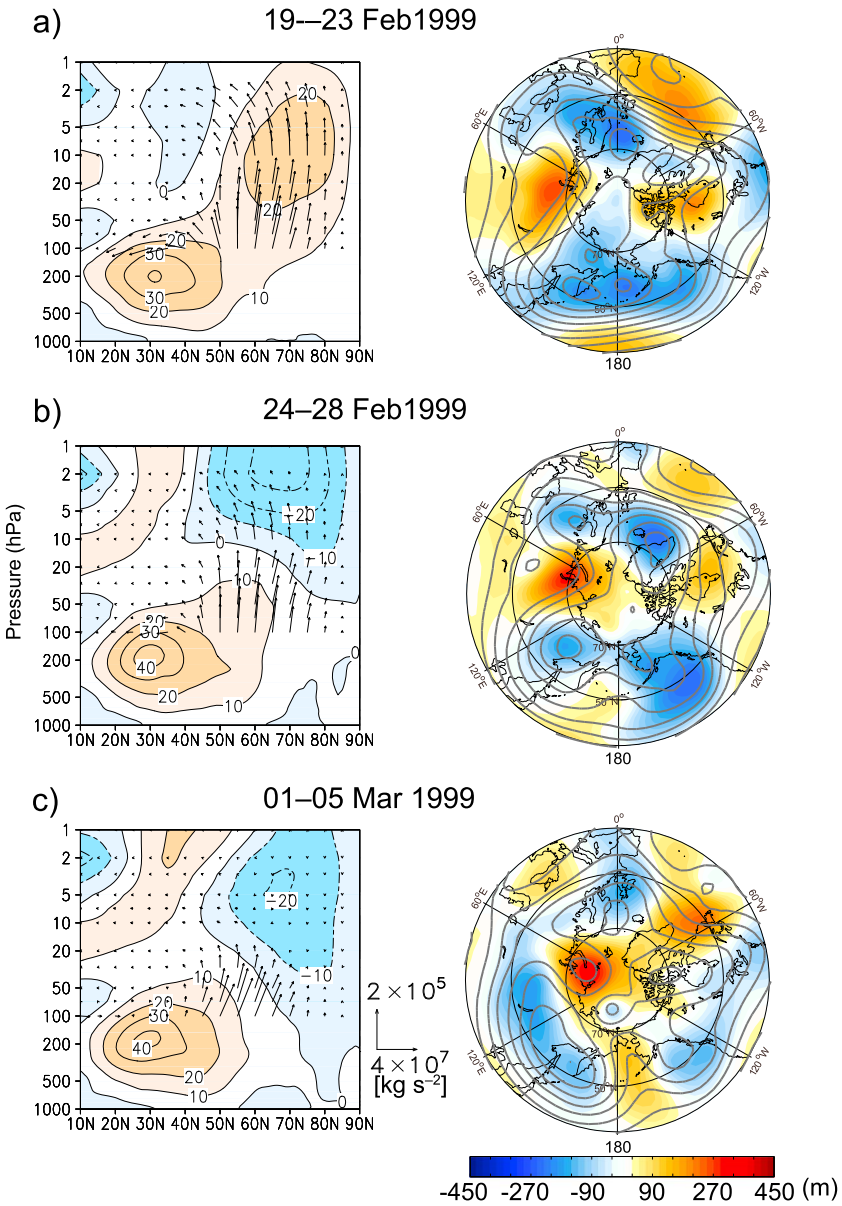

Figure 3. As in Figure 2 except for the dates (a) 19–23 February, (b) 24–28 February, and (c) 1–5 March 1999.

also known as the central date by *Charlton and Polvani* [2007]. Obviously, polar night jets are considerably weakened on the central dates; i.e., 15 December 1998 (Figure 2b) and 26 February 1999 (Figure 3b). In the case of December 1998, downward propagation of planetary waves occurs in the polar lower stratosphere soon after. As a consequence, the perturbed polar night jet starts to recover. However, in the case of February 1999, planetary wave activity declines, but waves continue to propagate upward and poleward in the lower stratosphere. Accordingly, the weaker polar night jet extends further downward.

It is noted in Figure 2 (right column) that the downward propagation of planetary waves in the December event precedes an amplification of planetary waves in the troposphere. Subsequently, the planetary-scale ridge over Alaska produces blocking, together with strong zonal flow over the North Atlantic, similar to those shown in a previous study [*Kodera et al.,* 2013]. In the case of the February 1999 SSW (Figure 3), downward extension of the weaker zonal wind creates a seesaw pattern between the polar region and the surrounding area in the geopotential height field.

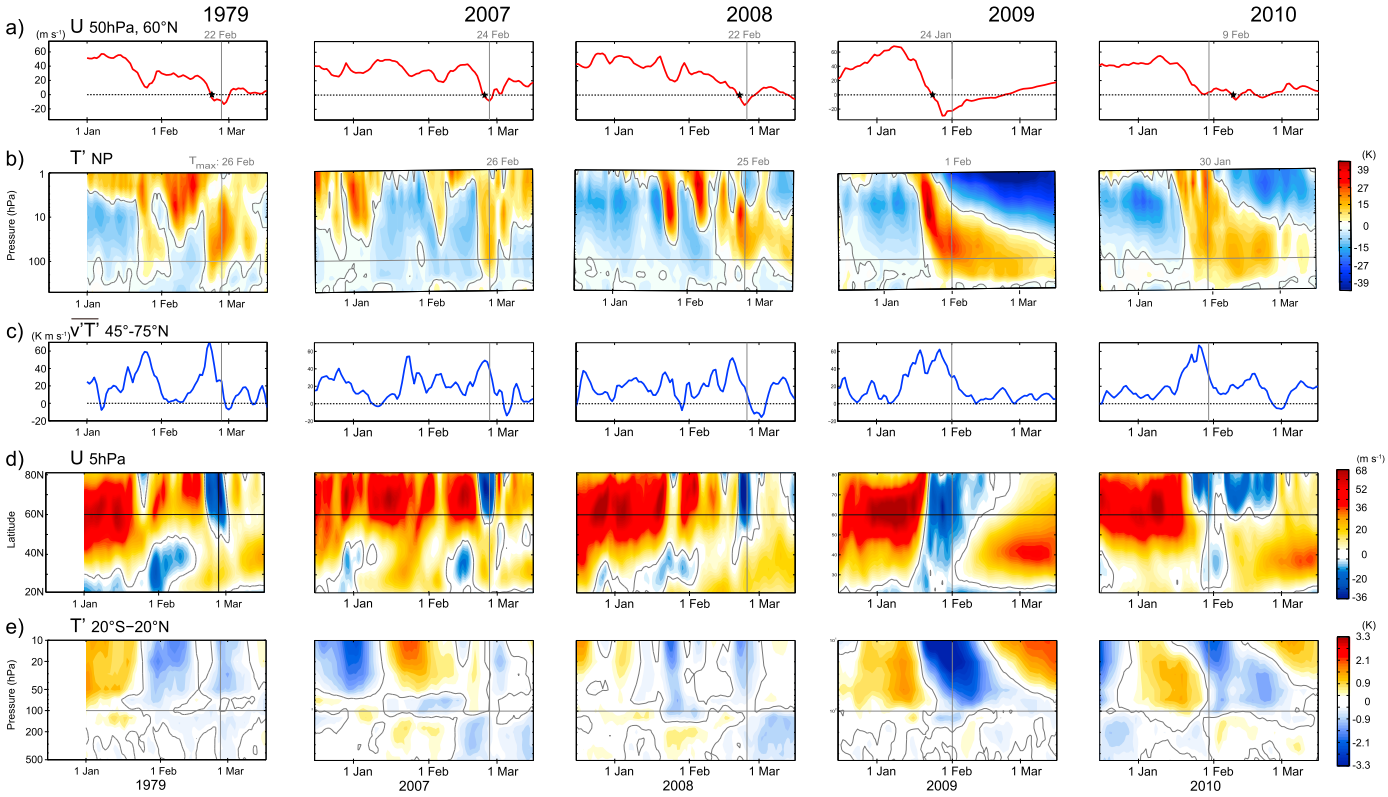

Figure 4. Evolution of atmospheric circulation between 16 December and 16 March, for the five years studied here. (a) 10 hPa zonal mean zonal wind at 60°N. Asterisks indicate the date of the appearance of the easterly wind, or the onset of major SSW. (b) Height-time section of anomalous temperature (deviation from the climatology) around the North Pole (80–90°N). Vertical lines indicate when the 50 hPa anomalous polar temperature attained a local maximum during an SSW event (T_{max}). (c) Eddy heat flux at 100 hPa averaged over 45–75°N. (d) Latitude-time section of 5 hPa zonal mean zonal wind. Zero lines are indicated by contours. (e) Height-time section of temperature anomalies averaged over the tropics (20°S–20°N). Here the anomaly is defined as a deviation from the climatology and the average over the illustrated period.

3.2. Winter 2007–2010 and 1979

Meteorological variables related to the SSW events are illustrated in Figure 4 for the three months from 16 December to 16 March in each boreal winter of 2007–2010 As distinct wave number 2 SSWs are rare [*Harada et al.,* 2010], we also examined the SSW event from February 1979, which is considered to be a typical event and has been investigated many times [*Andrews et al.,* 1987] but exhibits noticeably different characteristics from those seen in 2009 as will be shown later.

Figure 4a shows the time series of zonal mean zonal wind at 10 hPa and 60°N, and the onset date of the major SSW is indicated by an asterisk. The height-time section of the anomalous North Pole (80–90°N) temperature defined as a deviation from the climatology is shown in Figure 4b. Multiple short-term warmings in the upper stratosphere are prominent during the winters of 1979, 2007, and 2008. Conversely, the winters of 2009 and 2010 are characterized by a long-lasting deep warming following a period of cooling. The warming signal penetrates downward beneath 100 hPa for the SSWs in 2009 and 2010 but remains almost within the middle stratosphere for the other SSWs. The 10 hPa polar temperature rise for the minor warming around 24 January 2008 exceeds that observed in most of the major SSWs. It can be seen that the major SSW events are not necessarily characterized by a magnitude of the warming in the upper stratosphere, but a deep warming that extends into the lower stratosphere. In this respect, it is noted that, unlike others, *Limpasuvan et al.* [2004] define the SSWs using the zonal wind at the 50 hPa level.

In accordance with the polar temperature variation, the NH eddy heat flux at 100 hPa (Figure 4c) shows a shorter-term fluctuation during the winters of 1979, 2007, and 2008. The vertical solid lines show the date when the 50 hPa polar temperatures reach their maximum, T_{max}, which corresponds to the starting point of the recovery or end phase of the SSW. A particularly noticeable feature of these winters is that the eddy

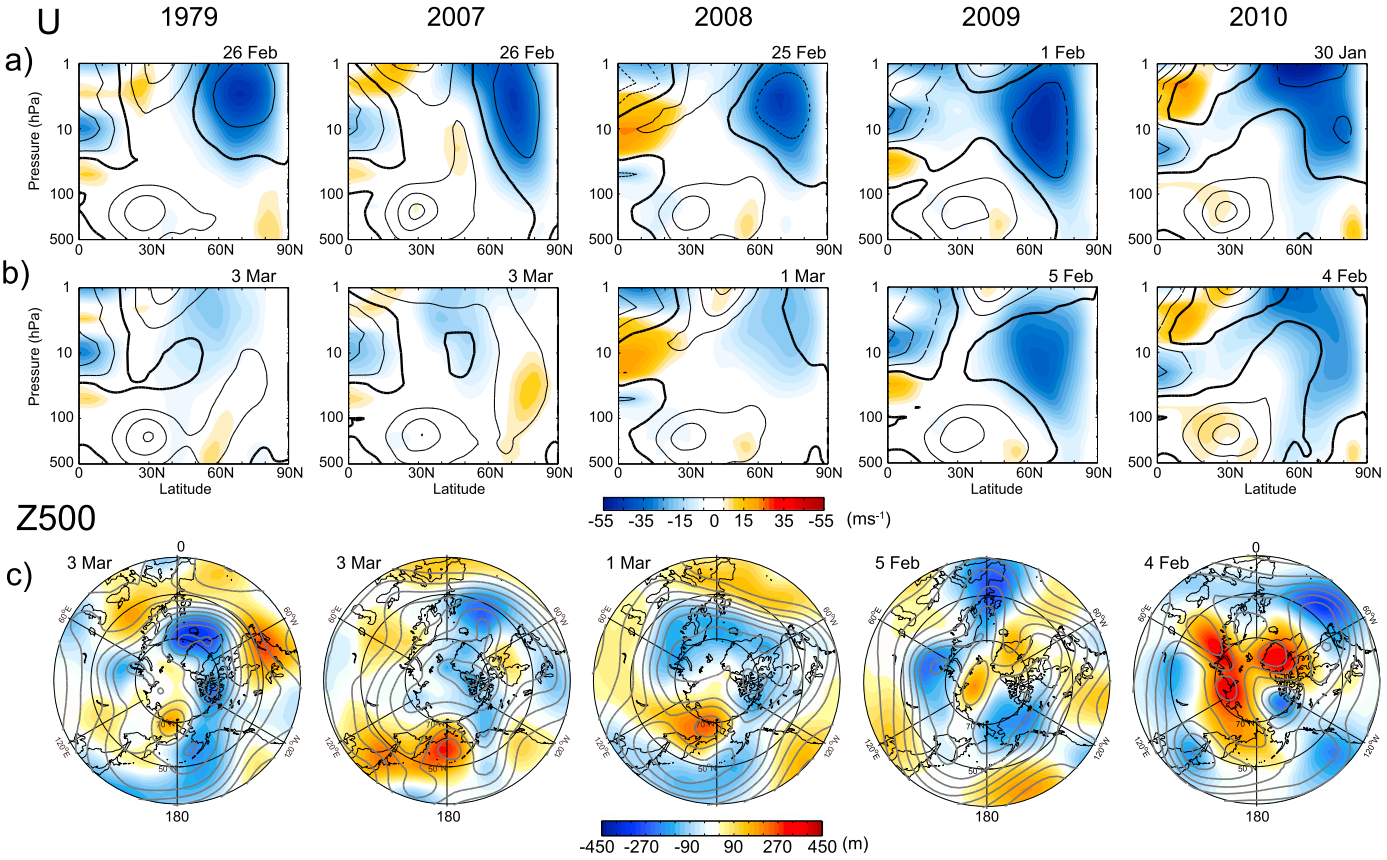

Figure 5. (a) Meridional sections of 5 day mean zonal mean zonal wind (contour interval is 15 m s^{-1}; zero contours shown by thick lines) and its anomaly with respect to the climatology (color shading) around T_{max} (vertical lines in Figure 4). The dates indicate central day of the 5 day period. (b) As in Figure 5a, except for 5 days later. (c) 500 hPa geopotential height (contour interval is 100 m) and its anomaly from the climatology (color shading) for dates shown in Figure 5b.

heat flux becomes negative after the warming peak. For the 2009 and 2010 events, the heat flux remains positive and decreases more gradually.

Another characteristic of these events is the meridional extent of the upper stratospheric circulation change associated with the SSW. Figure 4d shows a latitude-time section of the 5 hPa zonal mean zonal wind. Despite a strong deceleration of westerlies in the polar region, weakening of the westerly was mostly confined to higher latitude regions for the SSWs in 1979, 2007, and 2008. In contrast, during the SSW events in 2009 and 2010, the deceleration of the westerly occurred over a wider latitudinal range extending from the subtropics to the polar region, which induced a large-scale hemispherical meridional circulation. Consequently, strong cooling occurred in the tropical stratosphere during these events. However, it is much less conspicuous for the SSWs in 1979, 2007, and 2008 (Figure 4e).

Figure 5 depicts the temporal evolution of the circulation during the recovery phase. Zonal mean zonal wind (contours) and its deviation from the climatology (color shading) are shown for each event around T_{max} and also 5 days later. Westerly winds are weakened and the polar night jet has disappeared from the upper stratosphere around T_{max} in all cases (Figure 5a), whereas differences between the events have become apparent 5 days later (Figure 5b). The westerly jet recovers in the stratosphere for the SSWs in 1979, 2007, and 2008. This is associated with a downward propagation of planetary waves as depicted in the 3 day mean E-P flux sections in Figure 6. For the SSWs in 2009 and 2010, the weakening of zonal winds descends from the lower stratosphere further into the troposphere (Figure 5b). The corresponding 500 hPa geopotential height is displayed in Figure 5c. A seesaw pattern of the anomalous geopotential height between the polar and surrounding regions, a characteristic of the negative AO phase, is seen for the SSWs in 2009 and 2010, consistent with negative zonal wind anomalies in the polar tropospheric region (Figure 5b). For the SSWs in 1979, 2007, and 2008, blocking around the Aleutian-East Siberia sector and an intensified zonal flow

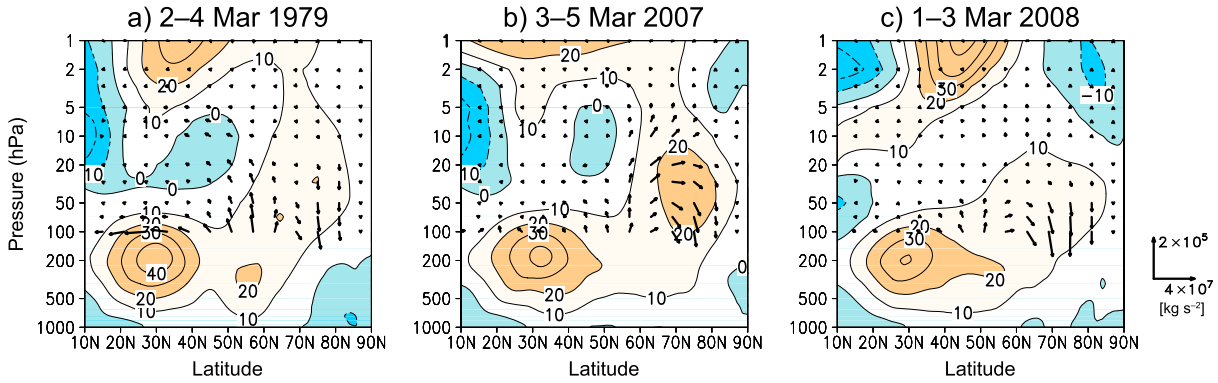

Figure 6. Meridional cross sections of 3 day mean E-P flux sections with zonal mean zonal wind during the recovery phase for (a) 2–4 March 1979, (b) 3–5 March 2007, and (c) 1–3 March 2008.

pattern over the North Atlantic sector in the troposphere attract our attention. Such a tropospheric circulation pattern is similar to that observed to be associated with planetary wave reflection in the stratosphere by *Kodera et al.* [2013].

3.3. Zonal Wave Structure and Polar Vortex

In the above analysis, we showed that the major difference between the SSWs in December 1998 and February 1999 arises from distinct vertical propagation of the planetary waves during the recovery phase. *Nakagawa and Yamazaki* [2006], however, attributed the different tropospheric impacts of these two SSWs to the geometry of the deformed polar vortex, but without detailed analysis. Therefore, we will examine the relationship between the polar vortex and the wave structure during these events in detail. To capture rapid evolution of the structure related to the change in wave propagation, 3 day mean is used in the following analysis. Geopotential height (contours) and relative vorticity (color shading) fields at 10 hPa are shown in the top panels in Figure 7. The left- and right-hand panels are for the SSW in December 1998 and February 1999, respectively. Figures 7a and 7c show the 3 day means around the central date, and Figures 7b and 7d are those for seven days later. The height-longitude sections of the zonally asymmetric component of geopotential height averaged over 60–70°N are shown around the central date (Figures 7e and 7f), and 7 days later (Figures 7g and 7h). Note that the origin of the abscissa (longitude) has been shifted to the region where tropospheric planetary waves propagate upward: the Atlantic for 1998 and Eurasia for 1999 events.

The polar vortex on the central date is displaced from the North Pole for the SSW in December 1998 (Figure 7a), whereas that for the SSW in February 1999 (Figure 7c) has two centers, consistent with the splitting-type SSW classified by *Charlton and Polvani* [2007]. Such a difference in the geometry of the polar vortex is related to the difference in the spatial structure of the wave packet (Figures 7e and 7f). In both cases, trough and ridgelines tilt westward as altitude increases, suggesting upward and eastward propagation. The difference between the two events arises from the difference in wavelength and phase of the wave packets: two troughs are found at 10 hPa for the SSW in February 1999, but only one is seen for the SSW in December 1998.

A more important difference in the wave structure occurs in the following period. The tilt of trough and ridgelines reverses from westward to eastward with increasing altitude for the SSW in December 1998 (Figure 7g) consistent with a change in the vertical propagation direction of E-P flux from upward to downward (Figure 2). In the case of the SSW in February 1999, the westward tilt is maintained (Figure 7h) through the continuous upward propagation (Figure 3). The shape of the polar vortex also evolves with the change in the vertical propagating property of the wave packets. The polar vortex of the SSW in December 1998 also splits into two parts (Figure 7b). Consequently, *Mitchell et al.* [2013] classified this SSW as a mix of both types, whereas they classified the SSW in February 1999 as a displacement type. For these SSWs, classification by the geometry of the polar vortex not only is ambiguous but also has no clear relationship with the 500 hPa geopotential height field. In contrast, the vertical propagation property of planetary waves in the stratosphere has a direct connection with the tropospheric response.

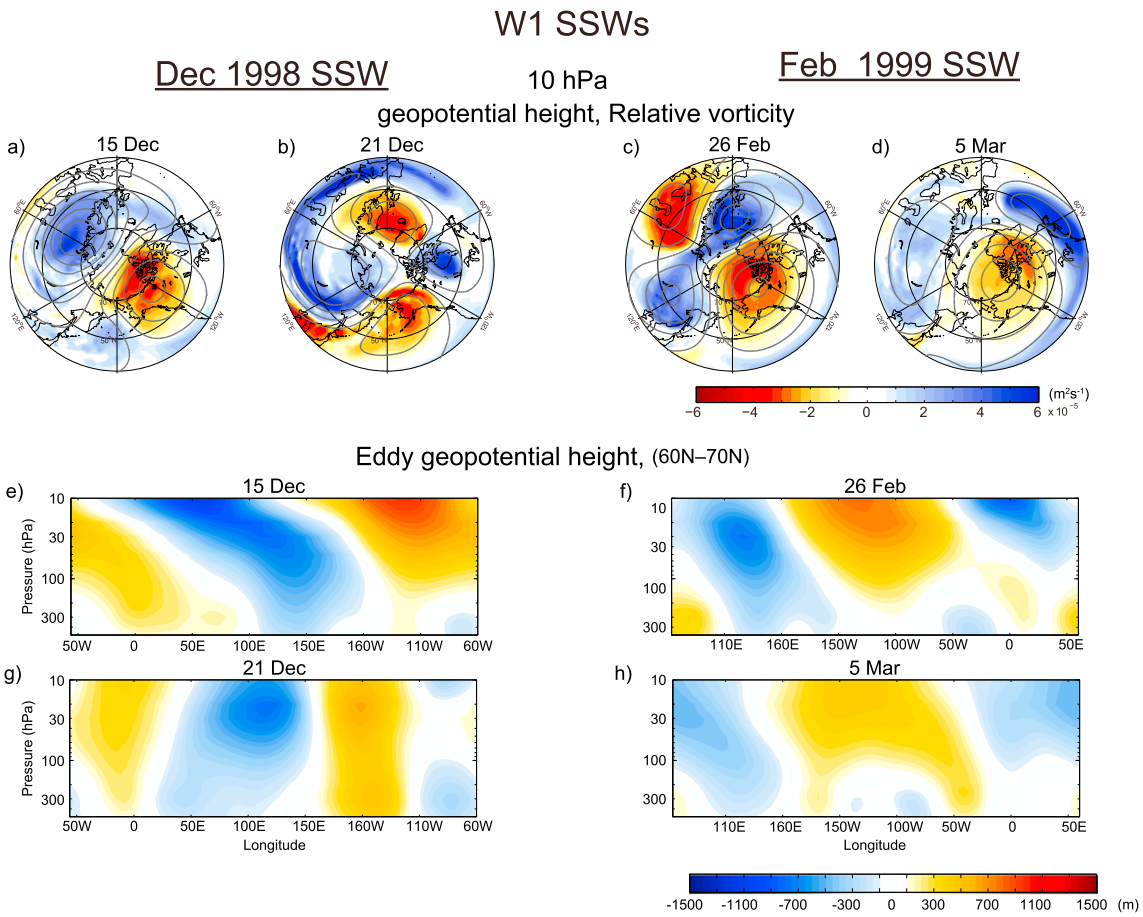

Figure 7. Wave number 1 SSW events for (a, b, e. and g) December 1998 and (c, d, f, and h) February 1999 events. (Figures 7a and 7b) Three-day mean geopotential height (contours) and relative vorticity (color shading) at 10 hPa. The dates indicate central day of the 3 day period. (Figures 7a and 7c) Period around the central date and (Figures 7b and 7d) 7 days later. (Figures 7e and 7f and 7g and 7h) Height-longitude sections of 3 day mean zonally asymmetric component of geopotential height averaged over 60–70°N. (Figures 7e and 7f) Period around central day and (Figures 7g and 7h) 7 days later.

Note that both events in the winter of 1999 can be classified as wave number 1 SSWs (Figure 1d). To investigate whether similar differences exist for wave number 2 warmings, the SSWs in 1979 and 2009 were also examined (Figure 8). In the beginning, as expected, two ridges and two troughs are found for these wave number 2 warmings, and they are both tilted westward with height in accordance with upward propagation. Although the amplitude diminishes, this structure is maintained after the central date for the 2009 SSW. However, in the case of the 1979 SSW, the tilt of the ridgeline with height becomes eastward due to the change in the direction of vertical propagation from upward to downward as seen in Figure 6. Note also that a ridge over Europe disappears in the stratosphere. Accordingly, in the 1979 SSW, one of the vortices at 10 hPa diminishes rapidly and a zonal wave number-1 feature emerges, whereas in 2009, two vortices persist during the recovery phase of the SSW.

3.4. Composite Mean

Although, more detailed results of the composite analysis on the SSW will be presented in a separate paper for stratospheric processes, here we show preliminary ones on the different tropospheric response to the SSW according to the present classification. First, we selected 22 SSW events during winters from 1980 to 2013 following the same criterion of *Charlton and Polvani* [2007] that the zonal mean zonal wind at 10 hPa, 60°N becomes easterly during 1 December to 31 March. The date when the 50 hPa polar temperature reaches its maximum, T_{max}, was taken as the key date. Then, they are classified according to the eddy heat flux associated with zonal wave number 1 and 2 components at 100 hPa averaged over 45°N–75°N: when the heat flux remains negative more than 2 days among 7 days on and after the T_{max} (day 0 to day 6), they were classified

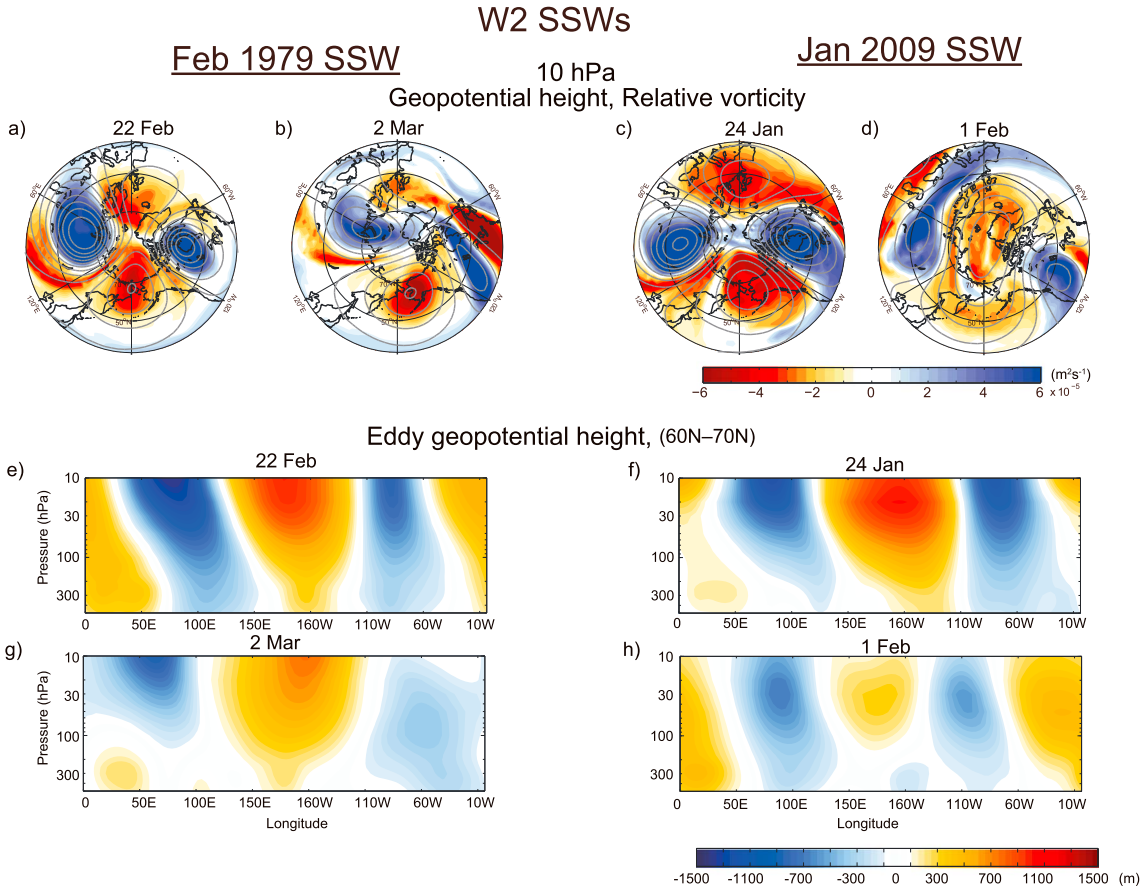

Figure 8. As in Figure 7 except for wave number 2 SSW events for (a, b, e, and g) February 1979 and (c, d, f, and h) January 2009 events. Figures 8a, 8c, 8e, and 8f are around the central date, and Figures 8b, 8d, 8g, and 8h are 8 days later.

as the reflecting type (nine cases). The rest (13 cases) was classified as the absorbing type. The key dates for each type are as follows: (reflecting type) 2 March 1980, 26 February 1984, 2 January 1985, 13 March 1988, 24 February 1989, 17 December 1998, 6 January 2004, 26 February 2007, and 25 February 2008 and (absorbing type) 2 March 1981, 4 December 1981, 5 February 1987, 12 December 1987, 5 March 1999, 11 February 2001. 2 January 2002, 18 January 2003, 15 March 2005, 25 January 2006, 1 February 2009, 30 January 2010, and 15 January 2013.

Figure 9a shows the composite mean evolution of the eddy heat flux associated with planetary waves 1 and 2. The composite means of the geopotential height at 500 hPa for the absorbing and reflecting types are shown in Figures 9b and 9c, respectively. Left- and right-hand panels show 6 day average for day 0 to 5, and day 5 to 10, respectively. Statistically significant regions are indicated in the supporting information (Figure S1). We can see that tropospheric response of the absorbing type for day 0 to 5 can be characterized by a negative AO-like pattern with positive anomalies around the polar region and negative ones in midlatitudes, whereas that of the reflecting type exhibits a deepening of trough over the North Atlantic and an enhancement of a ridge around the Aleutian sector, which confirms the result of case studies described above. The AO-like pattern of the absorbing type persists during the following period of day 5 to 10. However, the spatial structure of the reflecting type further evolves with time: positive anomalies over the central Pacific sector shift westward and reside over Eurasian continent.

To examine whether such tropospheric evolution during the reflecting-type SSW is associated with the downwelling of planetary waves in the stratosphere, we calculated the composite mean of 14 downwelling events of the zonal wave number 1 component defined irrespective to the occurrence of the SSW according to Table 1 in *Shaw and Perlwitz* [2013]. Zonal wave number 1 component of the geopotential height averaged over 60°N–70°N is shown in Figure 10a, while the zonal asymmetric component including all wave numbers is

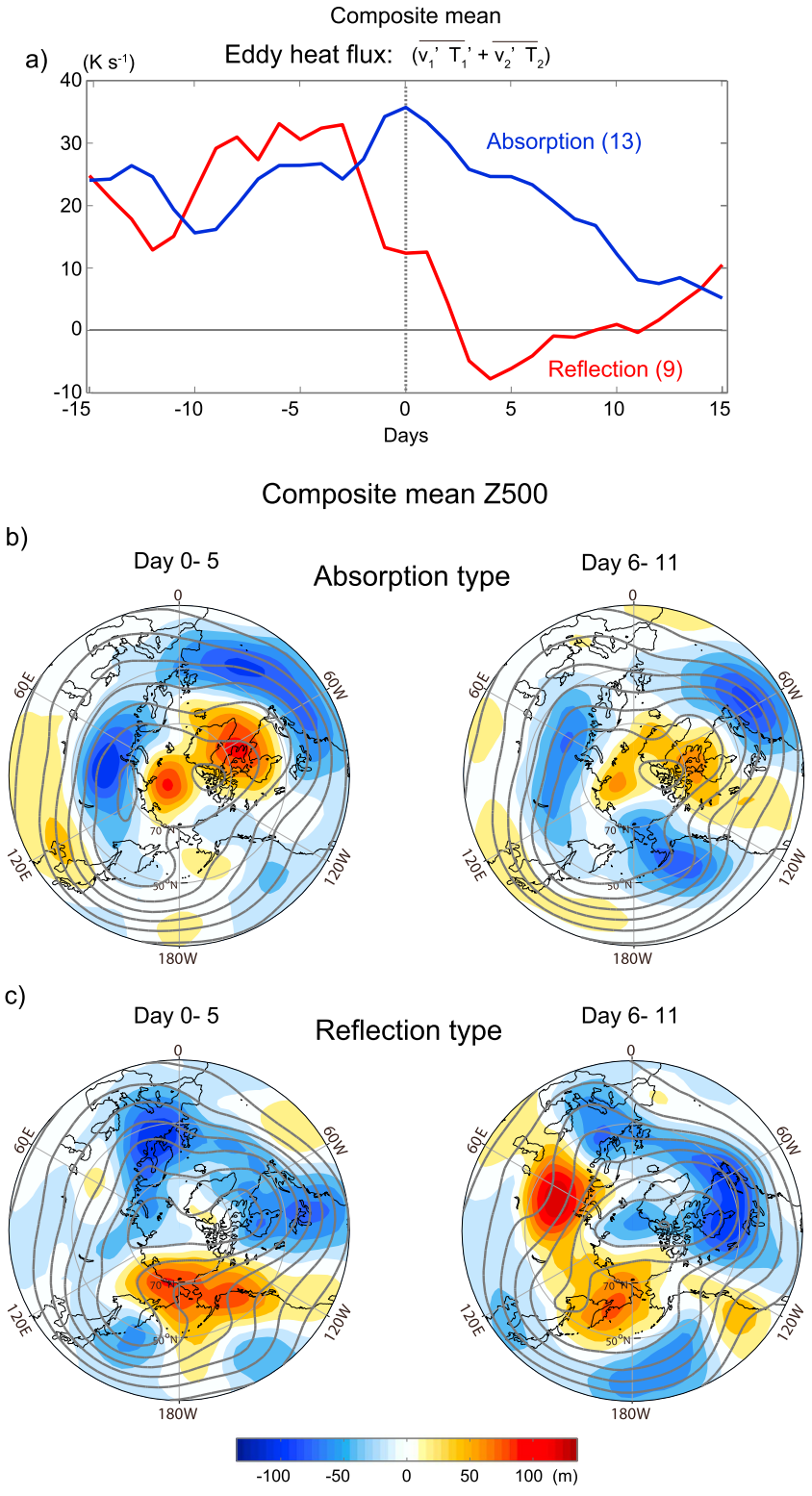

Figure 9. (a) Composite means of the eddy heat flux associated with zonal wave numbers 1 and 2 at 100 hPa averaged over 45–75°N for the absorbing (blue line) and reflecting-type (red line) SSWs. (b) Composite means of 500 hPa geopotential height (contour interval 100 m) and their anomalies from the climatology (color shading) for the absorbing type. Left- and right-hand panels are 6 day means for day 0 to 5 and day 5 to 10, respectively. (c) Same as in Figure 9b except for the reflecting type.

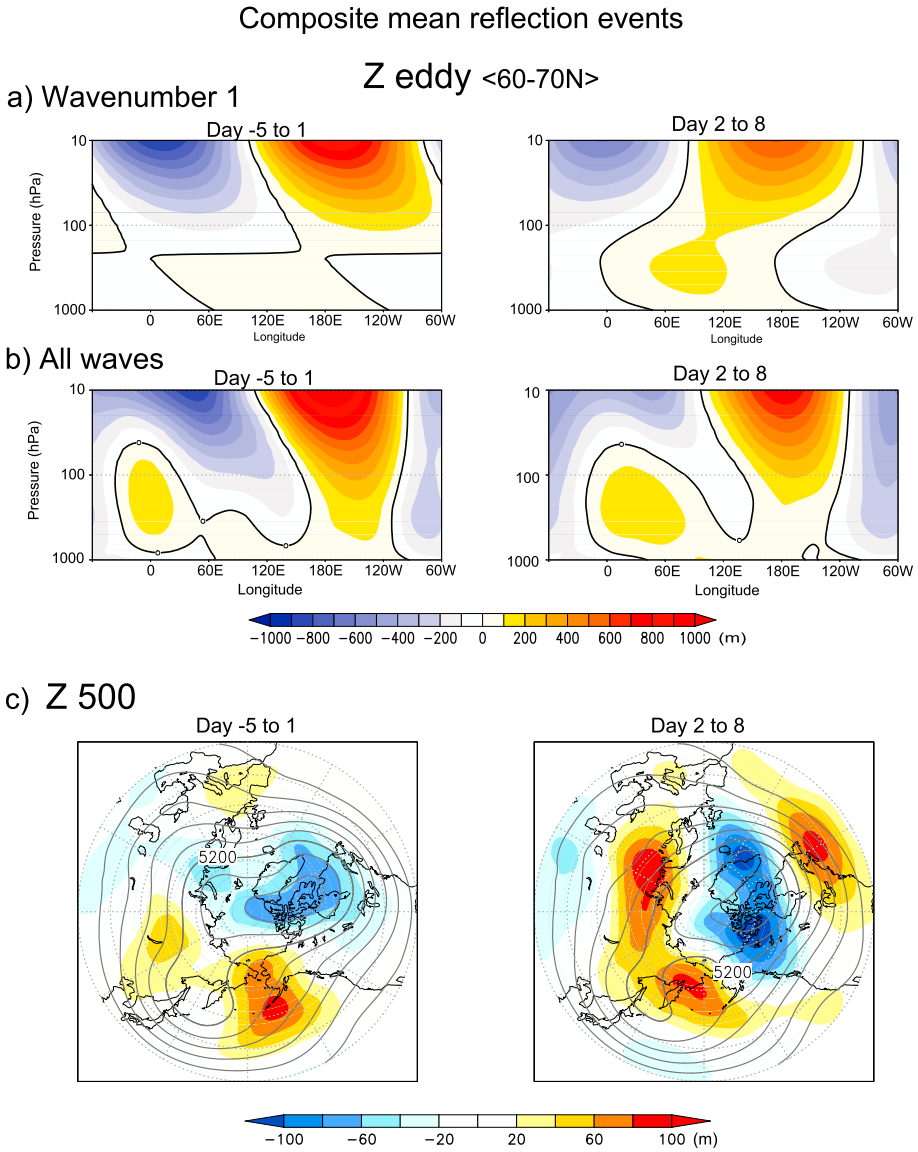

Figure 10. Composite mean of 14 wave number 1 reflection events selected according to Table 1 in *Shaw and Perlwitz* [2013]. (a) Composite mean of zonal wave number 1 component of geopotential height averaged over 60 N°–70°N: Day −5 to 1 (left) and day 2 to 8 (right). (b) Same as in Figure 10a except for the zonal asymmetric component including all wavenumbers. (c) Same as in Figure 10a, except for 500 hPa geopotential height (contour interval 100 m) and their anomalies from the climatology (color shading).

displayed in Figure 10b. Left- and right-hand panels are the means for day −5 to 1 and 2 to 8, respectively. Composite means of 500 hPa geopotential height of the same periods are also presented in Figure 10c. The trough line over the Eurasian sector tilts westward with increasing altitude, whereas that over the Atlantic sector tilts conversely to eastward for day −5 to 1 in Figure 10b. This means that a wave packet propagating upward from the Eurasian sector is reflected in the stratosphere and propagates downward in the American-North Atlantic sector, which leads to a development of a ridge over the central Pacific sector.

Because zonal wave number 1 component is not dominant, in order to identify its structural change the other components have to be removed. When we focus on wave number 1 component alone, stratospheric component is disconnected from tropospheric one at the beginning during day −5 to 1. When the reflection of wave number 1 component occurs on day 2 to 8, trough and ridge lines change the tilt from westward to eastward with increasing altitude and extend from the stratosphere to the troposphere (Figure 10a, right).

Accordingly, tropospheric ridge shifts westward and develops over the Eurasian continent (Figure 10c), similar to the composite map of the reflecting-type SSW in Figure 9c.

4. Discussions and Concluding Remarks

Our analysis of seven major SSW events indicates that the influence of SSW on the troposphere differs considerably according to whether or not reflection occurs during the recovery phase of the SSW. The common features for each type of SSW are summarized below.

For the absorbing type (such as the SSWs in February 1999, January 2009, and January 2010), the deceleration of zonal winds starts in the subtropical upper stratosphere. The decelerating zone shifts poleward from the subtropics and then the warming descends in the polar region. The poleward and downward penetration is similar to the polar night jet oscillation [*Kuroda and Kodera*, 2004]. In this respect, it is also noticeable that a cooling occurs prior to the SSW in the polar stratosphere in association with the strengthening of the polar night jet. The tropospheric response associated with this type of SSW appears through changes in the polar night jets, and thus appears as a negative AO-like pattern.

For the reflecting type (the SSWs in February 1979, December 1998, February 2007, and February 2008.), the deceleration of stratospheric zonal winds is confined mainly to the polar region. Warming is rapidly terminated by reflection of planetary waves, which induces downward propagation of the wave packets. Fluctuations, including intermittent warming periods, precede or follow the major warming. The tropospheric response of this type of SSW appears as an amplification of the tropospheric planetary wave in the recovery phase of the SSW. In particular, a deepening trough over the North Atlantic and an enhancing ridge in the North Pacific sector are evident. The latter enhancement provides a favorable condition for a blocking formation over the North Pacific.

The classification of SSW events proposed in this study is based on the propagation property of planetary waves and focuses on the temporal evolution of the stratospheric circulation during the recovery phase of the SSW. In contrast, the conventional classification using the dominant zonal wave number focuses on the developing phase of the SSW, whereas classification by the geometry of the polar vortex is based on its mature phase. *Charlton and Polvani* [2007] stated that, although vortex splits and vortex displacements have substantially different structures in the stratosphere, their integrated hemispheric impact on the troposphere is broadly similar. In fact, the tropospheric connection is more directly related to the vertical structure of planetary waves than the horizontal structure of the polar vortex as shown in Figures 7 and 8. Thus, the proposed classification of the SSW is directly relevant to the influence of the SSW on tropospheric circulation.

No direct comparison has been undertaken with results by *Mitchell et al.* [2013] who claim that stratospheric vortex splitting have stronger annular responses in the tropospheric circulation than displacement SSWs. This is because, unlike in *Charlton and Polvani* [2007] where events are selected according to a conventional criterion that the zonal mean wind at 10 hPa, at 60°N becomes easterly, there is no such constrain in the strength of the zonal winds, nor polar temperature variation. As a matter of fact, among the 40 events selected by *Mitchell et al.* [2013] in their Table 1, only 10 cases (25%) agree with those classified by *Charlton and Polvani* [2007].

Harnik [2009] and *Shaw and Perlwitz* [2010] considered that both the reflection associated with the downward propagation of planetary waves in the stratosphere and the SSW event occur following the upward propagation of planetary waves to the upper stratosphere, and they are complementary. *Harnik* [2009] argued that the reflection occurs in the upper stratosphere because of the shorter duration of the incoming wave pulse compared with the SSW event. The present study shows that the reflection also occurs in the middle or lower stratosphere during a recovery phase of the SSW, even if the duration of the incoming pulse is sufficiently long to cause the major warming.

According to the linear theory, the zonal wave number spectrum is conserved and the basic flow is invariant during the reflection event. The reflection events in the upper stratosphere and stratopause region are well described by a quasi-linear model: waves decelerate zonal winds in the upper stratosphere and form a reflecting surface [e.g., *Harnik and Lindzen*, 2001, *Harnik,* 2009]. However, both zonal winds and the zonal wave number spectrum may evolve during the SSW event. The SSW in February 1979 is a typical example of such a highly nonlinear case in which the dominant component of the upward propagating wave is wave number 2, but that

of the downwelling wave is wave number 1 (Figure 8), which might be generated by wave-wave interaction in the stratosphere [*Smith et al.,* 1984; *Jung et al.,* 2001]. In fact, among the downward propagating events associated with the wave number 1 component listed in *Shaw and Perlwitz* [2013], the largest negative vertical component of the wave number 1 E-P flux occurs during the wave number 2 SSW event in February 1979.

Here we used the term reflection to describe the downward propagation of planetary waves following the upward propagation because the waves subsequently return. However, in a highly nonlinear case, the term reemission would also be appropriate. Nevertheless, the tropospheric response of this wavenumber 2 February 1979 event has similar spatial characteristics to the mean composited wave number 1 reflection events, i.e., a developed trough over the North Atlantic and a pronounced ridge around the Aleutian-Kamchatka region (compare Figure 5c with Figure 10c). Note also that stratospheric wave number 1 component in Figure 10a (left) is disconnected from that in the troposphere before the reflection starts. Hence, it is suggested that the impact of the downwelling planetary wave on the tropospheric circulation does not depend on how it is generated.

The dynamical behavior of mechanistic models of SSW can be well understood within the framework proposed in this study. The mechanistic model used in *Matsuno* [1971] was constructed such that planetary waves are absorbed in the equatorial stratosphere. Hence, it produces the characteristic poleward movement of negative zonal mean zonal wind anomalies from the tropics, which in turn initiates the SSW. This behavior is similar to that observed for the absorbing type of SSW. In the case of the mechanistic model of *Holton and Mass* [1976], waves are allowed to propagate only vertically, so that they are easily trapped due to the upper stratospheric zonal wind configuration. The trapping of planetary waves in the polar region is an important and necessary condition for the wave reflection. In this sense stratospheric vacillation in their model would correspond to multiple pulses in reflecting-type SSWs.

There is a tendency for the subtropical jet in the upper stratosphere to be stronger in the reflecting SSWs (Figure 5a). It is known that planetary wave propagation is particularly sensitive to the latitudinal profile of zonal mean zonal winds in the tropical regions [*Yoden and Ishioka*, 1993; *Gray*, 2003]. Taking account this relationship, we may infer that the subtropical upper stratospheric zonal wind would play a key role in determining whether a SSW event will evolve subsequently as the absorbing or reflecting type. More detailed analysis, based on a larger number of SSW events, will be necessary to examine this hypothesis in a future study.

Acknowledgments

The ERA-Interim atmospheric reanalysis data have been obtained from ECMWF (http://www.ecmwf.int/en/research/climate-reanalysis/era-interim). This work was supported in part by the Japanese Ministry of Education, Science, Sports and Culture via Grants-in-Aid for Scientific Research (S)24224011. P. Maury and C. Claud acknowledge the support of the French National Research Agency (ANR) through the StraDyVariUS project, ANR-13-BS06-0011. The authors would like to thank the reviewers for providing valuable detailed comments.

References

Andrews, D. G., J. R. Holton, and C. B. Leovy (1987), *Middle Atmosphere Dynamics*, 489 pp., Academic, Orlando, Fla.

Ayarzagüena, B., U. Langematz, and E. Serrano (2011), Tropospheric forcing of the stratosphere: A comparative study of the two different major stratospheric warmings in 2009 and 2010, *J. Geophys. Res.*, *116*, D18114, doi:10.1029/2010JD015023.

Baldwin, M. P., and T. J. Dunkerton (1999), Propagation of the Arctic oscillation from the stratosphere to the troposphere, *J. Geophys. Res.*, *104*, 30,937–30,946, doi:10.1029/1999JD900445.

Baldwin, M. P., and T. J. Dunkerton (2001), Stratospheric harbingers of anomalous weather regimes, *Science*, *294*, 581–584.

Bancalá, S., K. Krüger, and M. Giorgetta (2012), The preconditioning of major sudden stratospheric warmings, *J. Geophys. Res.*, *117*, D04101, doi:10.1029/2011JD016769.

Barriopedro, D., and N. Calvo (2014), On the relationship between ENSO, stratospheric sudden warmings, and blocking, *J. Clim.*, *27*, 4704–4720.

Castanheira, J. M., and D. Barriopedro (2010), Dynamical connection between tropospheric blockings and stratospheric polar vortex, *Geophys. Res. Lett.*, *37*, L13809, doi:10.1029/2010GL043819.

Charlton, A. J., and L. M. Polvani (2007), A new look at stratospheric sudden warmings. Part I: Climatology and modeling benchmarks, *J. Clim.*, *20*, 449–469.

Cohen, J., and J. Jones (2011), Tropospheric precursors and stratospheric warmings, *J. Clim.*, *24*, 6562–6572.

Dee, D. P., et al. (2011), The ERA-Interim reanalysis: Configuration and performance of the data assimilation system, *Q. J. R. Meteorol. Soc.*, *137*, 553–597.

Eguchi, N., K. Kodera, and T. Nasuno (2015), A global non-hydrostatic model study of a downward coupling through the tropical tropopause layer during a stratospheric sudden warming, *Atmos. Chem. Phys.*, *15*, 297–304, doi:10.5194/acp-15-297-2015.

Gómez-Escolar, M., N. Calvo, D. Barriopedro, and S. Fueglistaler (2014), Tropical response to stratospheric sudden warmings, *J. Geophys. Res. Atmos.*, *119*, 7382–7395, doi:10.1002/2013JD020560.

Gray, L. J. (2003), The influence of the equatorial upper stratosphere on stratospheric sudden warmings, *Geophys. Res. Lett.*, *30*(4), 1166, doi:10.1029/2002GL016430.

Harada, Y., A. Goto, H. Hasegawa, N. Fujikawa, H. Naoe, and T. Hirooka (2010), A major stratospheric sudden warming event in January 2009, *J. Atmos. Sci.*, *67*, 2052–2069.

Harnik, N. (2009), Observed stratospheric downward reflection and its relation to upward pulses of wave activity, *J. Geophys. Res.*, *114*, D08120, doi:10.1029/2008JD010493.

Harnik, N., and R. S. Lindzen (2001), The effect of reflecting surfaces on the vertical structure and variability of stratospheric planetary waves, *J. Atmos. Sci.*, *58*, 2872–2894.

Holton, J. R., and C. Mass (1976), Stratospheric vacillation cycles, *J. Atmos. Sci.*, *33*, 2218–2225.

Jung, J.-H., C. S. Konor, C. R. Mechoso, and A. Arakawa (2001), A study of the stratospheric major warming and subsequent flow recovery during the winter of 1979 with an isentropic vertical coordinate model, *J. Atmos. Sci.*, *58*, 2630–2649.
Kodera, K. (2006), Influence of stratospheric sudden warming on the equatorial troposphere, *Geophys. Res. Lett.*, *33*, L06804, doi:10.1029/2005GL024510.
Kodera, K., H. Mukougawa, and S. Itoh (2008), Tropospheric impact of reflected planetary waves from the stratosphere, *Geophys. Res. Lett.*, *35*, L16806, doi:10.1029/2008GL034575.
Kodera, K., H. Mukougawa, and A. Fujii (2013), Influence of the vertical and zonal propagation of stratospheric planetary waves on tropospheric blockings, *J. Geophys. Res. Atmos.*, *118*, 8333–8345, doi:10.1002/jgrd.50650.
Kodera, K., B. M. Funatsu, C. Claud, and N. Eguchi (2015), The role of convective overshooting clouds in tropical stratosphere–troposphere dynamical coupling, *Atmos. Chem. Phys.*, *15*, 6767–6774, doi:10.5194/acp-15-6767-2015.
Kuroda, Y., and K. Kodera (2004), Role of polar-night jet oscillation on the formation of the Arctic Oscillation in the Northern Hemisphere winter, *J. Geophys. Res.*, *109*, D11112, doi:10.1029/2003JD004123.
Kuttippurath, J., and G. Nikulin (2012), A comparative study of the major sudden stratospheric warmings in the Arctic winters 2003/2004–2009/2010, *Atmos. Chem. Phys.*, *12*, 8115–8129.
Limpasuvan, V., D. W. J. Thompson, and D. L. Hartmann (2004), The life cycle of the Northern Hemisphere sudden stratospheric warmings, *J. Clim.*, *17*, 2584–2596.
Martineau, P., and S.-W. Son (2013), Planetary-scale wave activity as a source of varying tropospheric response to stratospheric sudden warming events: A case study, *J. Geophys. Res. Atmos.*, *118*, 10,994–11,006, doi:10.1002/jgrd.50871.
Martius, O., L. M. Polvani, and H. C. Davies (2009), Blocking precursors to stratospheric sudden warming events, *Geophys. Res. Lett.*, *36*, L14806, doi:10.1029/2009GL038776.
Matsuno, T. (1971), A dynamical model of the stratospheric sudden warming, *J. Atmos. Sci.*, *28*, 1479–1494.
Mitchell, D. M., L. J. Gray, J. Anstey, M. P. Baldwin, and A. J. Charlton-Perez (2013), The influence of stratospheric vortex displacements and splits on surface climate, *J. Clim.*, *26*, 2668–2682.
Nakagawa, K. I., and K. Yamazaki (2006), What kind of stratospheric sudden warming propagates to the troposphere?, *Geophys. Res. Lett.*, *33*, L04801, doi:10.1029/2005GL024784.
Naujokat, B., K. Krüger, K. Matthes, J. Hoffmann, M. Kunze, and K. Labitzke (2002), The early major warming in December 2001—Exceptional?, *Geophys. Res. Lett.*, *29*(21), 2023, doi:10.1029/2002GL015316.
Nishii, K., H. Nakamura, and Y. J. Orsolini (2011), Geographical dependence observed in blocking high influence on the stratospheric variability through enhancement and suppression of upward planetary-wave propagation, *J. Clim.*, *24*, 6408–6423.
Perlwitz, J., and N. Harnik (2003), Observational evidence of a stratospheric influence on the troposphere by planetary wave reflection, *J. Clim.*, *16*, 3011–3026.
Perlwitz, J., and N. Harnik (2004), Downward coupling between the stratosphere and troposphere: The relative roles of wave and zonal mean processes, *J. Clim.*, *17*, 4902–4909.
Scherhag, R. (1952), Die explosionsartigen Stratosparenerwarmungen des Spatwinters 1952, *Ber. Dtsch. Wetterdienstes U. S. Zone*, *38*, 51–63.
Shaw, T. A., and J. Perlwitz (2010), The impact of stratospheric model configuration on planetary-scale waves in Northern Hemisphere winter, *J. Clim.*, *23*, 3369–3389.
Shaw, T. A., and J. Perlwitz (2013), The life cycle of northern hemisphere downward wave coupling between the stratosphere and troposphere, *J. Clim.*, *26*, 1745–1763.
Smith, A. K., J. C. Gille, and L. V. Lyjak (1984), Wave–wave Interactions in the stratosphere: Observations during quiet and active wintertime periods, *J. Atmos. Sci.*, *41*, 363–373.
Taguchi, M. (2011), Latitudinal extension of cooling and upwelling signals associated with stratospheric sudden warmings, *J. Meteorol. Soc. Jpn.*, *89*, 571–580.
Thompson, D. W. J., and J. M. Wallace (2001), Regional climate impacts of the Northern Hemisphere annular mode, *Science*, *293*(5527), 85–89.
Ueyama, R., E. P. Gerber, J. M. Wallace, and D. M. W. Frierson (2013), The role of high-latitude waves in the intraseasonal to seasonal variability of tropical upwelling in the Brewer–Dobson circulation, *J. Atmos. Sci.*, *70*, 1631–1648.
Woollings, T., A. J. Charlton-Perez, S. Ineson, A. G. Marshall, and G. Masato (2010), Associations between stratospheric variability and tropospheric blocking, *J. Geophys. Res.*, *115,* D06108, doi:10.1029/2009JD012742.
Yoden, S., and K. Ishioka (1993), A numerical experiment of the breakdown of polar vortex due to forced Rossby waves, *J. Meteorol. Soc. Jpn.*, *71*, 59–72.